14B.1 WRF MODEL STUDY OF THE GREAT PLAINS LOW-LEVEL JET: EFFECTS OF GRID SPACING AND BOUNDARY LAYER PARAMETERIZATION

Elizabeth N. Smith*, Jeremy A. Gibbs, Evgeni Fedorovich, and Timothy A. Bonin
School of Meteorology, University of Oklahoma, Norman, Oklahoma

1. Introduction

The nocturnal low-level jet (NLLJ) is defined as a wind maximum occurring overnight in the lowest kilometer of the atmosphere. In the U.S., NLLJs form commonly over the Great Plains; these jets are typically southerly and most often occur during the warm months of late spring, summer, and early autumn. According to the NLLJ climatology presented by Bonner (1968), the average height of NLLJ wind maxima is about 800 meters above ground level. More recently, Whiteman et al. (1997) showed that half of NLLJs occurring over the Great Plains have wind maxima below 500 meters. These wind maxima can be very strong, reaching speeds that are 70% higher than the previous day's geostrophic wind speed (Shapiro and Fedorovich 2010). NLLJs in the Great Plains are of meteorological importance due to their influence on weather and climate over the region (Stensrud 1996). Moisture transport from the Gulf of Mexico northward over the central U.S. by NLLJs has been related to the observed nocturnal maximum in warm-season rainfall recorded over the central U.S. (Markowski and Richardson 2011). Also, thermodynamic and dynamic support can be provided by LLJs for the initiation of deep convection and severe weather (Shapiro and Fedorovich 2009). Strong wind shear associated with NLLJs can be hazardous for aviation especially during takeoffs and landings. Beyond the aforementioned practical interests, NLLJs are of theoretical interest as fluid dynamical phenomenon due to the peculiarity of physical mechanisms associated with NLLJ formation.

Improving the prediction of nocturnal meteorological processes requires investigation of large and small scale factors that control the structure of the stable boundary layers (SBL) in which NLLJs form and associated improvement in model parameterizations. Current parameterization schemes are often inadequate especially when applied to the SBL. The deficiencies can be attributed at least in part to insufficient understanding of turbulent exchange processes in the SBL (Steeneveld 2008). Previous studies have extended our understanding of the NLLJ through investigations with numerical models. Zhong et al. (1996) showed that soil moisture changes impacted the jet amplitude and drier soils lead to stronger NLLJs. Pan et al. (2004) described the role of slope-induced horizontal temperature gradients in the formation of the NLLJ. However, it has been shown that the SBL and the NLLJ are not well captured by numerical models. The consistent underestimation of the magnitude and depth of the NLLJ was revealed by Storm et al. (2009) in a study using WRF with a variety of boundary layer parameterization schemes. Steeneveld et al. (2008) found similar results simulating the NLLJ with three state-of-the-art mesoscale models.

Simulation of the NLLJ with a mesoscale model is a useful exercise in understanding the phenomenon. Validation of the model's performance is a necessary step in the simulation process. High quality observations are necessary for comparison with simulations to gain insight into the ability of a model to accurately represent the NLLJ. In this work, the Weather Research and Forecasting (WRF; Skamarock et al. 2005) model predictions are compared to observations from recent field campaigns.

The Lower Atmospheric Boundary Layer Experiment (LABLE) took place at the Southern Great Plains Atmospheric Radiation Measurement program's facility near Lamont, Oklahoma (Klein et al. 2015). Among many other instruments, LABLE deployed a Doppler lidar which observed NLLJs during 2012. One NLLJ observation is shown in fig. 1 from 24 October 2012. These observations provide high resolution information about NLLJs at fifteen-minute temporal resolution which allow for validation of the model simulations. Similar observation methods were employed during the Plains Elevated Convection at Night (PECAN) field campaign during June and July 2015 permitting

* *Corresponding author address:* Elizabeth Smith, School of Meteorology, 120 David L Boren Blvd, Suite 5900, Norman, OK, 73072
Email: elizabeth.n.smith@ou.edu

similar analyses to be performed on NLLJs observed in the PECAN domain.

In the following sections the model setup will be described first. The impact horizontal and vertical grid spacing has on the simulated NLLJ will be analyzed. Next, the effect of different WRF planetary boundary layer schemes will be examined for this application.

2. Model setup

The Advanced Research WRF model version 3.6.1 was used for all analyses discussed herein. While some model options were changed between the experiments, other settings remained constant throughout the study. Initial and boundary condition data were derived from North American Mesoscale (NAM) Reanalysis on a 12-km grid. The boundaries were updated every 6 hours. Microphysics were parameterized using the WRF single moment 5-class scheme. The 2D Smagorinsky scheme was applied in lateral directions while cumulus parameterization was turned off. The Noah surface model was used. Radiation was accounted for via the RRTM longwave scheme and the Dudhia shortwave scheme. The model domain was centered over the Lamont, OK ARM measurement location.

The model was run from 1200 UTC on 23 October 2012 to 12 UTC on 24 October 2012. The first 12 hours of the simulation were treated as spin-up time and are not included in the analysis. While additional spin-up time is always desired, testing longer periods of spin-up time showed that beyond 12 hours differences are not apparent. This is likely partially due to the decoupling of the atmosphere from the surface during stable conditions.

3. Grid spacing

3.1 Horizontal grid spacing

Testing the horizontal grid spacing required otherwise identical simulations on 1-, 2-, and 4-km spaced grids. The vertical grid spacing in these simulations was as the WRF default vertically stretched grid. The tests were run on both a fixed physical grid (the number of grid points changed depending on the spacing) and a fixed numerical grid (the physical domain expanded with increased grid spacing).

The wind field from the simulation run on the 1-km grid is shown in fig. 2. On the 1-km grid, WRF underestimates the magnitude of the NLLJ. This underestimation is enhanced in the core of the jet. The temporal evolution and the structure of the jet is poorly captured on this grid as well. Results are marginally improved on the 2-km grid shown in fig. 3, but the underestimation of the magnitude of the NLLJ is still quite large. The worst underestimation is still in the core region, but the zone of poorest performance is smaller than for the 1-km grid. The temporal evolution of the NLLJ is better captured by the 2-km grid than the 1-km grid. The estimation of the structure of the jet is also improved on the 2-km grid especially earlier in the period of interest. Finally, the 4-km grid offers improved results over both the 1- and 2-km grids as shown in fig. 4. The NLLJ magnitude is still underestimated, but not to the same degree as with 1- and 2-km grid spacing. The largest underestimation is still in the core of the jet. The temporal resolution and the structure of the jet is better captured on the 4-km grid than on the 1- or 2-km grids.

These tests lead to the conclusion that simulations with the 4-km horizontal grid spacing offered best results compared to observations. Further reducing the grid spacing degrades the resulting fields. This finding is consistent with previous studies. Gibbs et al. (2011) found 4-km horizontal grid spacing to be the most appropriate option simulating the convective boundary layer. Kain et al. (2008) and Schwartz et al. (2009) both found finer structures produced by WRF with the 2-km horizontal grid spacing did not add enough value to the forecasts provided by 4-km WRF to justify the computational cost increase.

3.2 Vertical grid spacing

It would be intuitive to assume that additional vertical levels should improve the WRF-modeled NLLJ. This assumption was tested by comparing the WRF default stretched vertical grid to grids with 40- and 20-m vertical spacing in otherwise identical WRF simulations. A comparison of the vertical grids is shown in fig. 5.

The default WRF vertical grid employs terrain-following eta-levels which are stretched such that more vertical levels are located near the surface, and the spacing becomes larger higher up in the atmosphere. In the default configuration, this results in ten vertical levels within the lowest 2 km. The modified vertical grids use constant vertical spacing similar to a vertical grid commonly used in large eddy simulations (LES; references…). The 40-m grid has 101 levels in the vertical while the 20-m grid has 201 levels in the vertical. Such grids do cause a sacrifice in model top height; this is not a concern in the case of interest because no convection or strong updrafts persisted in the

simulation. In a case of stronger convection, updrafts impinging on the upper boundary would be a cause for concern. Imposing some type of physically justified vertical stretching in the levels above the boundary layer is a subject of future work to lift the model top.

Although the 4-km horizontally spaced grid was identified as the best option, vertical spacing tests were run on both the 1- and 4-km horizontally spaced grids for completeness. As discussed before, the default vertically stretched grid leads to underestimation of the magnitude of the NLLJ. This underestimation is most prevalent in the core of the jet. Simulations on the default vertically stretched grid can also miss important features in the temporal evolution and the structure of the NLLJ. Utilization of the 40-m vertically spaced grid, as shown in fig. 6, still leads to underestimation of the NLLJ, but does improve over simulations with the default vertically spaced grid. The largest underestimation is still in the immediate vicinity of the jet, but this zone of larger underestimation is smaller than in the simulation using the default vertically stretched grid. The increased number of vertical levels yielded an improved realization of the temporal evolution of the NLLJ. The improvement is also observed in the structure of the jet. The 40-m vertically spaced grid simulation resembles the observations much more closely. Simulations with the 20-m vertically spaced grid in fig. 7 produce very similar results to the simulations with 40-m vertically spaced grid. The estimation of the magnitude could be argued to be slightly improved with the 20-m grid over the 40-m grid. The temporal evolution and the structure of the jet are consistent with the observations, but show no obvious improvement over the structure and temporal evolution obtained with the 40-m grid.

In all cases, the 20- and 40-m spaced vertical grids offer improvement over the default stretched grid; however, the differences between the 20-m and the 40-m results are too small to be accurately quantified. Even if the 20-m vertical grid could produce quantitatively better results than the 40-m vertical grid, the large increase in computing time as a result of the restricted time step is arguably not practical. For these reasons, the 40-m vertically spaced grid was chosen as the optimal grid. This result was also found for simulations with both the 1- and 4-km horizontally spaced grids.

3.3 Boundary conditions

Boundary conditions are provided to the model every 6 hours from the 12-km NAM reanalysis dataset. In the previous discussion, all simulations maintained 256 grid points in each of the horizontal directions. This means the 1-km horizontally spaced grid spanned 256 km region while the 4-km horizontally spaced grid covered a 1024 km region. To see if the changing proximity of the boundaries to the point of interest has an impact on the result of the simulation, the 4-km 256-point simulation (1024 km across) was compared to a 1-km 1024-point simulation (1024 km across) with results shown in fig. 8. As would be expected, simulations on the 1024-point domain are much more expensive to run. The 1-km 1024-point simulation does perform better than the 1-km 256-point simulation. Simulations with the 4-km 256-point domain still produce better results than those the 1-km 1024-point domain. This implies that proximity to the boundary definitively plays a role in the degradation of the wind field from 4-km to 1-km grids, but other effects still support the conclusion that the 4-km grid is a better option over the 1-km grid.

Nested grids have not been used in the simulations discussed so far. This means the 12-km NAM reanalysis data used for initial and boundary conditions is downscaled differently to match the 4-km grid than to match the 1-km grid. To evaluate the impact this downscaling may have on the resulting wind fields, a 1-km horizontally spaced grid was nested within a 4-km horizontally spaced grid. Results from corresponding simulations are shown in fig. 9. The wind field resulting from The 1-km nested domain simulation very closely matches the 4-km 40-m domain simulation. Simulations with 1-km nested and 4-km domains misrepresent the jet in the same areas the same ways, but the 4-km domain simulation is a very slight improvement over the 1-km nested domain. Since the 1-km nested run performs nearly the same as the 4-km non-nested grid, using the 4-km 40-m domain appears to be the most efficient option.

4. Boundary layer parameterizations

Representing processes in the lower troposphere adequately is important to the accuracy of the forecasts provided by a mesoscale model. In the boundary layer, the large range of scales of motion make direct simultaneous reproduction of all processes computationally impossible. To account for processes of boundary-layer scale WRF uses planetary boundary layer (PBL) parameterization schemes. While many PBL schemes account for boundary layer processes in different ways, one way to categorize these schemes would be into local and non-local schemes. Local closure

schemes only allow those vertical levels that are immediately neighboring a given point to directly impact the variables at that point. In a non-local closure scheme, multiple vertical levels within the boundary layer can directly impact the value of a variable at a grid point. Local schemes are often thought to offer some disadvantage for application to the PBL since localized maxima are not always representative of the state of the rest of the PBL. Non-local schemes are assumed to generally represent the largest eddies better than local schemes and thus better represent deep PBL circulations. However, these characterizations of local and non-local closure schemes may not be relevant for more stable boundary layers. Changes in performance in schemes in the SBL can be attributed – at least partly – to insufficient understanding and thus crude parameterization of turbulent exchange processes in the SBL. Three PBL schemes from WRF were evaluated for application to the SBL and NLLJ. A local scheme (Mellor-Yamada Nakaniski Niino – MYNN), a non-local scheme (Yonsei University – YSU) and a local scale elimination scheme (Quasi-Normal Scale Elimination – QNSE) were compared. The local closure scheme, MYNN, is of the 1.5 order with a prognostic TKE equation. It induces some extra mixing to deal with poor local approximation of fluxes based on eddy diffusivity. Non-local YSU is of the first order. It directly specifies the eddy diffusivity and has explicit treatment of entrainment processes. Lastly, QNSE is classified as a local closure of the 1.5 order with a prognostic TKE equation. It uses the scale elimination approach to better approximate exchange by turbulent eddies. QNSE was developed specifically for the SBL.

Tests of the PBL schemes were run with all grid options for completeness, but results were consistent across all grids. In each test run, only the PBL scheme and associated surface scheme was altered to isolate effects to those due to the PBL scheme. When the MYNN scheme was used, the NLLJ could not develop in any of the considered cases. When ran on different horizontally and vertically spaced grids, the NLLJ either never developed at all, or if a jet did develop it was quickly mixed vertically through the boundary layer as shown in fig. 10. Similar findings in Olsen and Brown (2012) lead to the conclusion that MYNN has strong sensitivity to the parameters used in the scheme to estimate mixing length scale. Jahn et al. (2014) also saw this behavior from the MYNN scheme and suggested that the LES derived closure constants in the scheme may be unsuitable for some applications. Runs employing the YSU scheme fared much better than with MYNN runs. Most simulations discussed in section 3 used the YSU scheme. These simulations were found to underestimate the NLLJ magnitude, but can decently capture the temporal evolution and structure of the NLLJ when other settings are used optimally. Simulations employing the QNSE scheme perform comparably to the simulations with YSU, but there are notable improvements when using QNSE as shown in fig. 11. WRF simulations using QNSE more closely estimate the magnitude of the NLLJ. Over- and underestimates only consistently occur in the periods of jet development and decay and do not predominately occur in the core of the jet as was the case in the other configurations tested. The temporal evolution of the jet is well captured, which is consistent with the observations. The structure of the jet is also well captured, consistently with the observations.

5. Conclusions

The NLLJ simulated with the WRF model is sensitive to horizontal grid spacing with decreased horizontal spacing degrading the simulated wind field. While boundary effects do play a role in this degradation, they are not solely responsible for it. Tests indicate that 4-km horizontal spacing is the optimal choice for simulating the NLLJ. Vertical grid spacing is also important for better simulating the NLLJ using WRF. A uniformly spaced vertical grid offers large improvements over the default vertically stretched grid WRF uses. In the conducted tests, a 40-m spaced grid performs nearly as well as a 20-m spaced grid. With computational considerations in mind, the 40-m grid is the optimal choice for simulating the NLLJ.

The local MYNN PBL scheme severely underestimates and over-mixes the NLLJ. The nonlocal YSU scheme performs much better than MYNN and produces a NLLJ close to the one seen in the observations, but the jet magnitude is often underestimated. The local scale elimination used by the QNSE scheme results in the best resolved NLLJ. The magnitude of the jet is very well reproduced while the temporal evolution and structure of the jet are also well captured.

Based on presented analyses, the optimal grid on which to simulate the NLLJ in WRF was identified as a 4-km horizontally spaced and 40-m vertically spaced grid. The QNSE PBL scheme is the best suited scheme for NLLJ simulations. These options were employed in simulations of NLLJ cases observed during the PECAN field campaign. Preliminary data suggests that this configuration of

WRF is successful in simulating the NLLJ cases observed during PECAN. These validated mesoscale simulations will supplement the observed datasets by expanding the spatial and temporal extent of the data available during the PECAN cases.

6. References

Bonner, W. D., 1968: Climatology of the low-level jet. *Mon. Wea. Rev.*, **96 (12)**, 833-850.

Gibbs, J. A., E Fedorovich, and A. M. van Eijk, 2011: Evaluating WRF model predictions of turbulent flow parameters in a dry convective boundary layer. *J. Appl. Meteor. Climatol.*, **50 (12)**, 2429-2444.

Jahn, D. E., W. Gallus, E. S. Takle, 2014: Evaluation of the MYNN PBL scheme closure constants for low-level jet events in a stable boundary layer. Pro., AMS Boundary Layer Symposium 2014, Leeds, UK.

Kain, J. S., S. J. Weiss, D. R. Bright, M. E. Baldwin, J. J. Levit, G. W. Carbin, C. S. Schrawts, M. L. Weisman, K. K. Droegemeier, D. B. Weber, and K. W. Thomas, 2008: Some practical considerations regarding horizontal resolution in the first generation of operational convection allowing NWP. *Wea. Forecasting*, **23 (5)**, 931-952.

Klein, P., T. A. Bonin, J. F. Newman, D. D. Turner, P. B. Chilson, C. E. Wainwright, W. G. Blumberg, S. Mishra, M. Carney, E. P. Jacobson, S. Wharton, and R. K. Newsom, 2015: LABLE: a multi-institutional, student-led atmospheric boundary-layer experiment. *Bull. Amer. Meteor. Soc.*, **96 (10)**, 1743-1764.

Markowski, P. and Y. Richardson, 2011: *Mesoscale meteorology in midlatitudes*, Vol. 2. John Wiley and Sons.

Olsen J. and J. M. Brown, 2011: Modifications in the MYNN PBL/surface layer scheme for WRF-ARW. Pro., WRF Users Workshop 2012, Boulder, CO.

Pan, Z. M. Segal, and R. W. Arritt, 2004: Role of topography in forcing low-level jets in the central United States during the 1993 flood-altered terrain simulations. *Mon. Wea. Rev.*, **132 (1)**, 396-403.

Schwartz, C. S., J. S. Kain, S. J. Weiss, M. Xue, D. R. Bright, F. Kong, K. W. Thomas, J. J. Levit, and M. C. Coniglio, 2009: Next-day convection-allowing WRF model guidance: a second look at 2-km versus 4-km grid spacing. *Mon. Wea. Rev.*, **137 (10)**, 3351-3372.

Shapiro, A. and E. Fedorovich, 2009: Nocturnal low-level jet over a shallow slope. *Acta Geophys.*, **57 (4)**, 950-980.

Shapiro, A. and E. Fedorovich, 2010: Analytical description of a nocturnal low-level jet. *Q. J. Roy. Meteor. Soc.*, **136 (650)**, 1255-1262.

Skamarock, W. C., J. B. Klemp, J. Dudhia, D. O. Gill, D. M. Barker, W. Wanf, and J. G. Powers, 2005: A description of the Advanced Research WRF version 2. Tech. rep., DTIC Document.

Steeneveld, G., J. Vila-Guerau de Arellano, A. Holtslaq, T. Mauritsen, G. Svensson, and E. de Bruijn, 2008: Evaluation of limited-area models fro the representation of the diurnal cycle and contrasting nights in CASES-99. *J. Appl. Meteor. Climatol.*, **47 (3)**, 869-887.

Stensrud, D. J., 1996: Importance of low-level jets to climate. *J. Climate*., **9(8)**, 1698-1711.

Storm, B., J. Dudhia, S. Basu, A. Swift, and I Giammanco, 2009: Evaluation of the WRF model on forecasting low-level jets: implications for wind energy. *Wind Energy*, **12 (1)**, 81-90.

Whiteman, C. D., X. Bian, and S. Zhong, 1997: Low-level jet climatology from enhanced rawinsonde observations at a site in the Southern Great Plains. *J. Appl. Meteor.*, **36 (10)**, 1363-1376.

Zhong, S., J. D. Fast, and X. Bian, 1996: A case study of the Great Plains low-level jet using wind profiler network data and a high resolution mesoscale model. *Mon. Wea. Rev.*, **124 (5)**, 785.

7. Figures

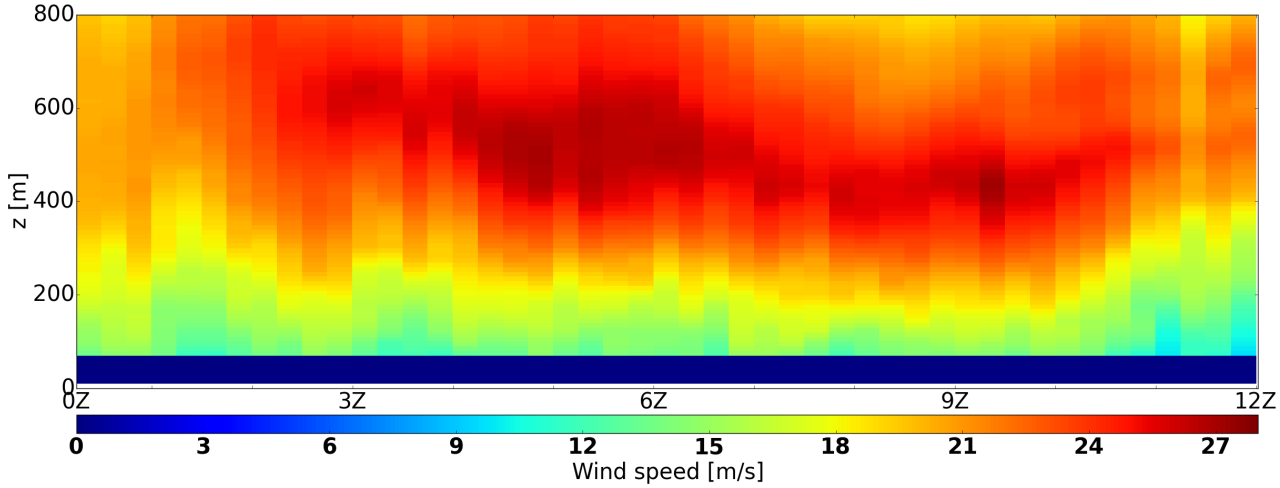

Figure 1. Lidar observations from the LABLE campaign shown a NLLJ that occured on 24 October 2012.

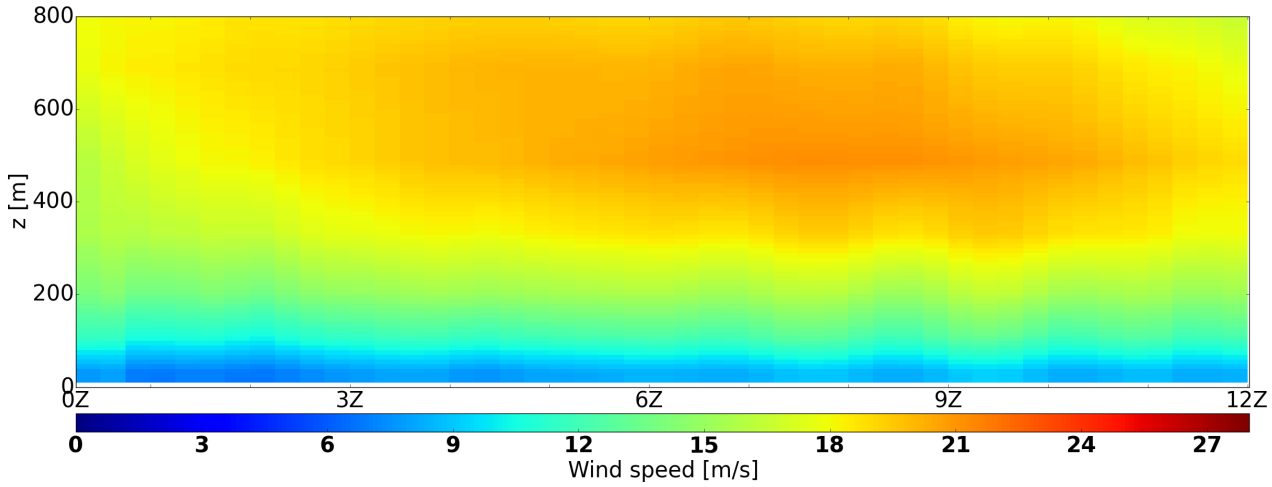

Figure 2. Wind fields from WRF simulation on a 1-km horizontally spaced and default stretched vertical grid.

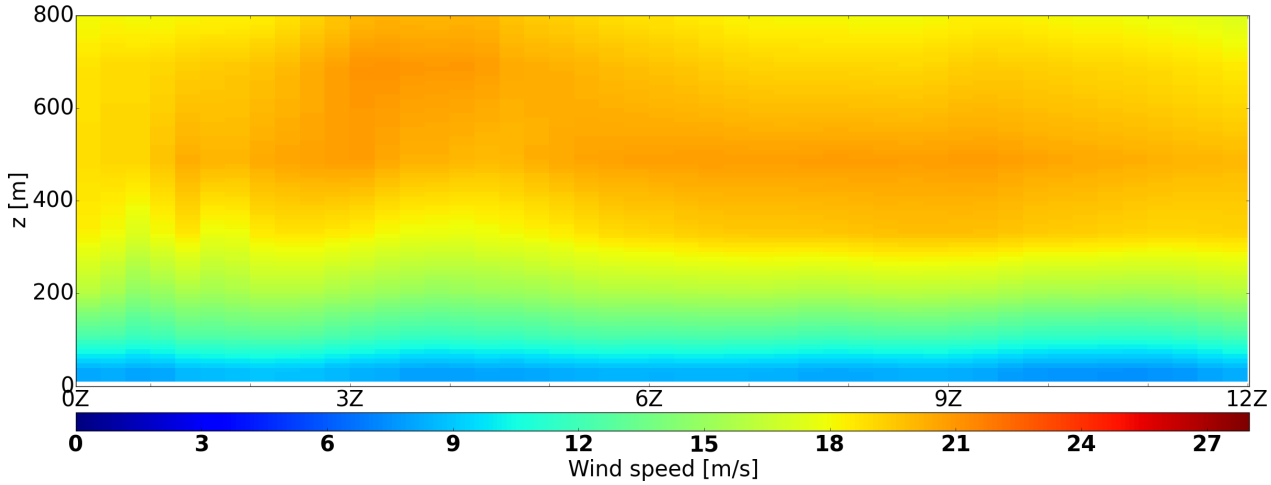

Figure 3. Wind field from WRF simulation on a 2-km horizontally spaced and default stretched vertical grid.

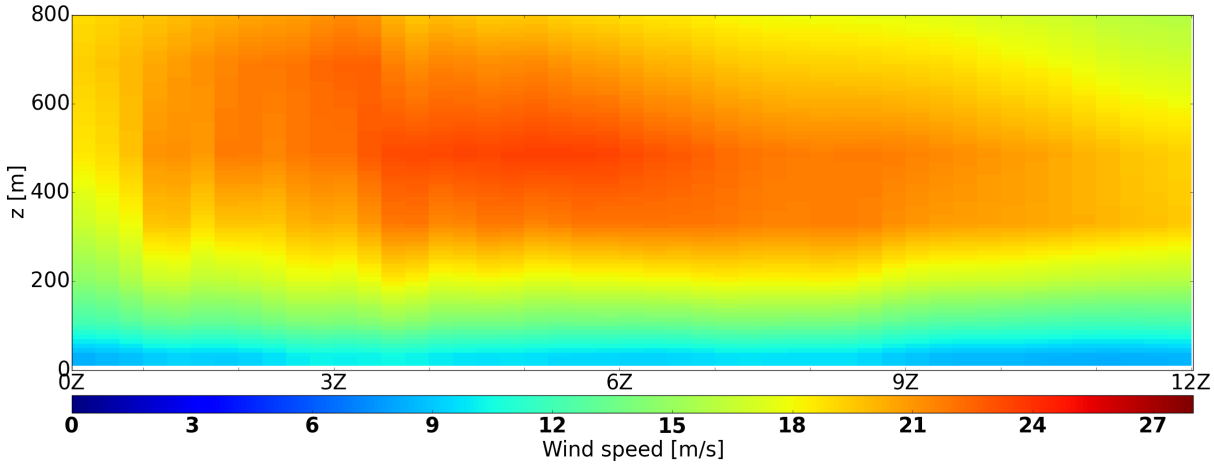

Figure 4. Wind field from WRF simulation on a 4-km horizontally spaced and default stretched vertical grid.

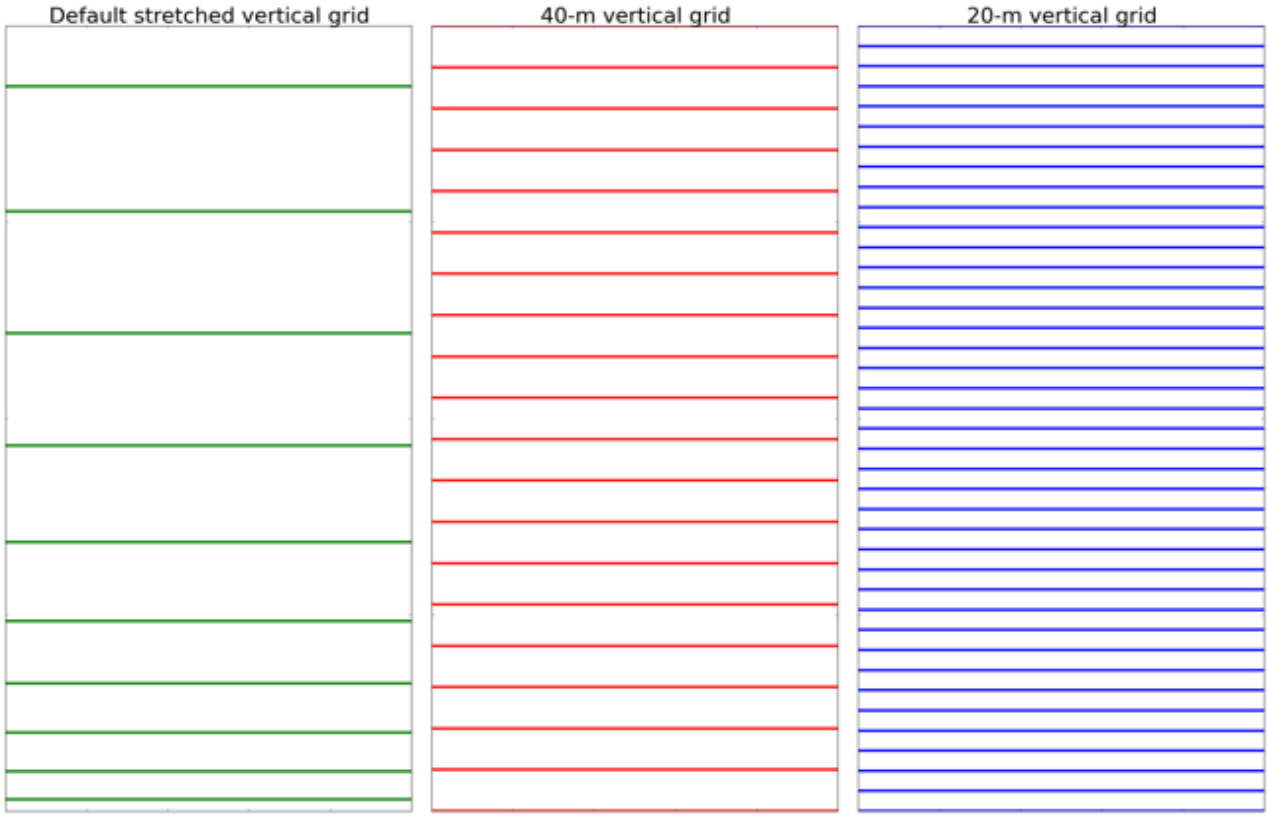

Figure 5. The default stretched vertical grid is shown compared to the 40-m and 20-m vertically spaced grids in the lowest 2-km of the atmosphere.

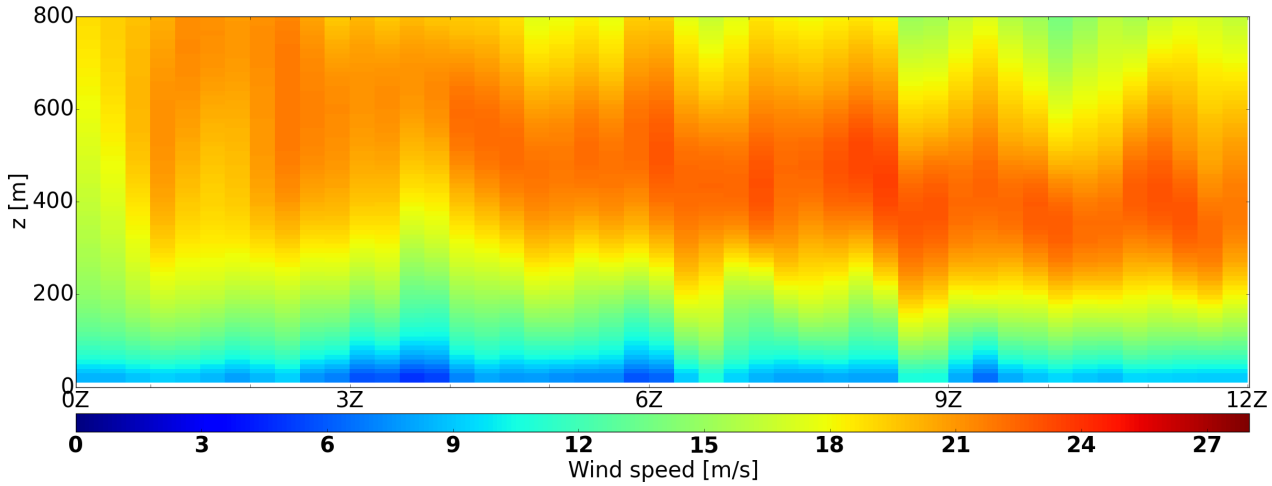

Figure 6. Wind field from WRF simulation on a 4-km horizontally spaced and 40-m vertically spaced grid.

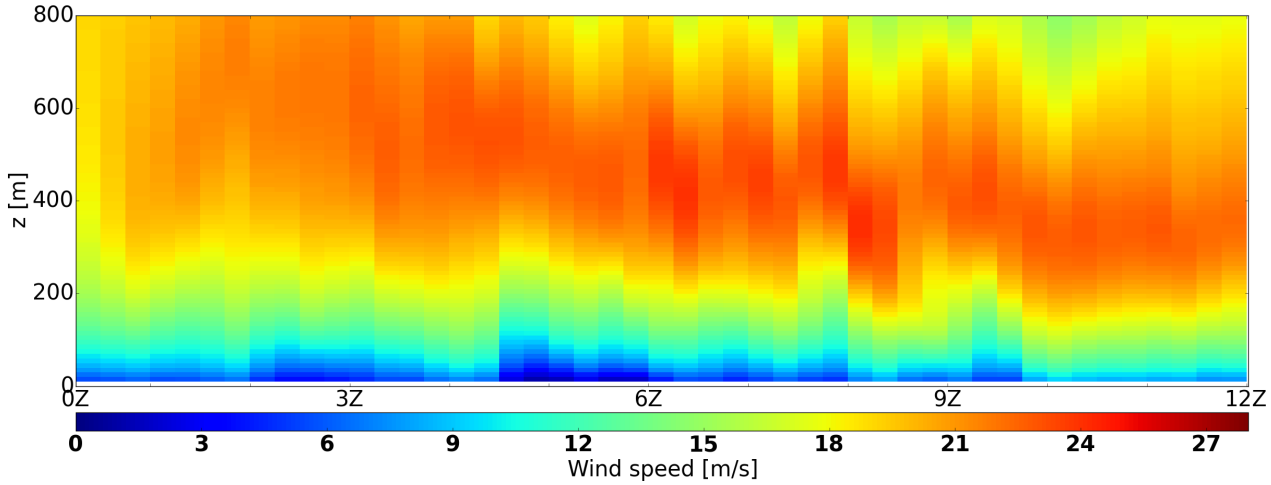

Figure 7. Wind field from WRF simulation on a 4-km horizontally spaced and 20-m vertically spaced grid.

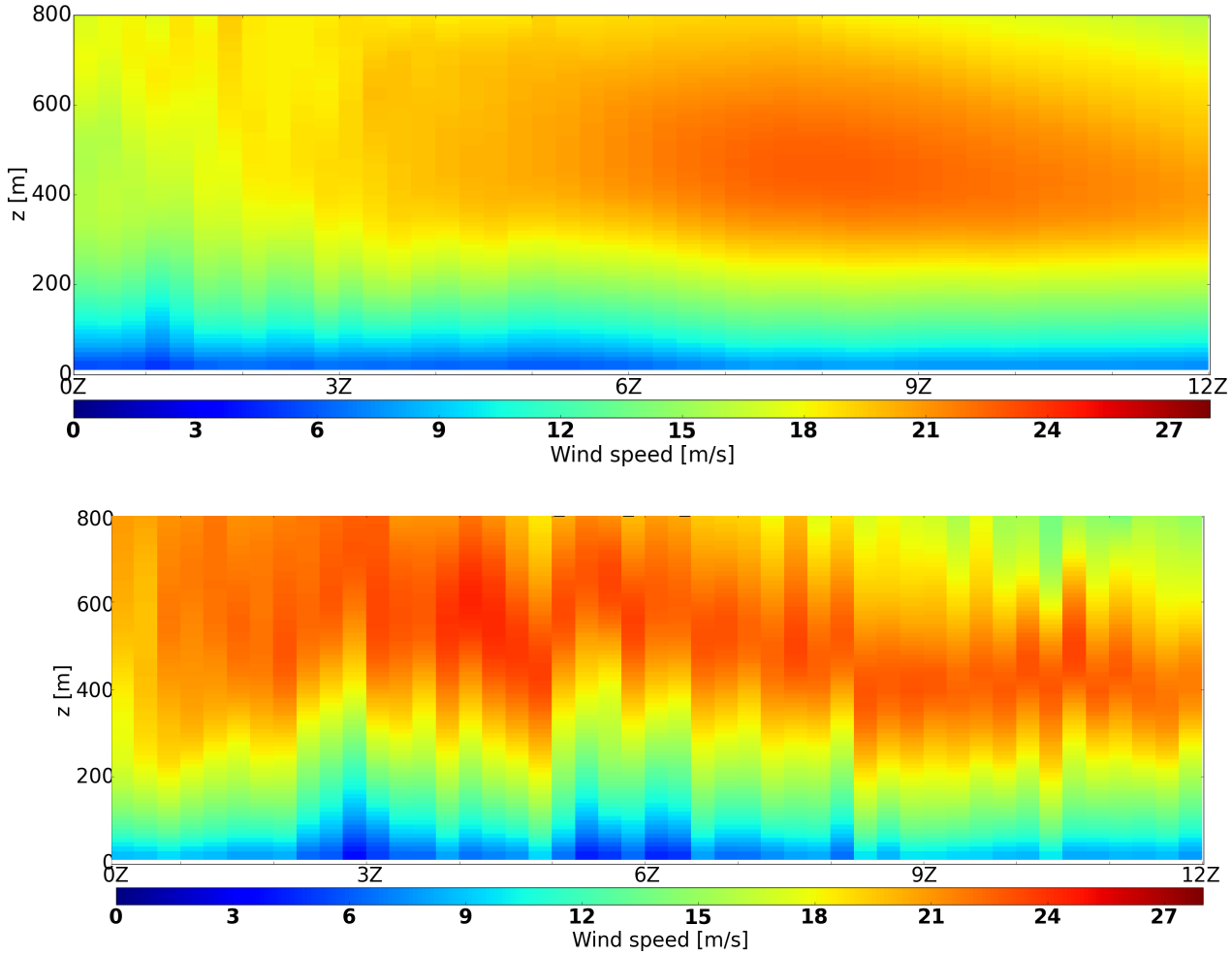

Figure 8. In the top panel, WRF simulation is shown on a 1-km horizontally spaced and 40-m vertically spaced grid with 256x256 points. The bottom panel shows a WRF simulation on a similarly spaced grid but with 1024x1024 points.

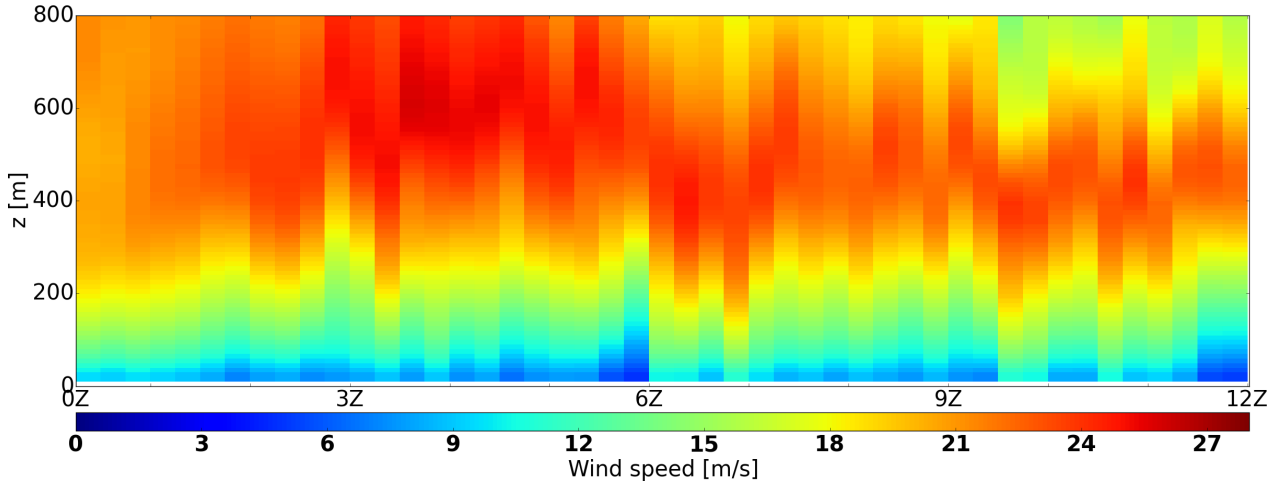

Figure 9. Wind field from WRF simulation on a 1-km horizontally spaced and 40-m vertically spaced grid nested in a 4-km horizontally spaced grid.

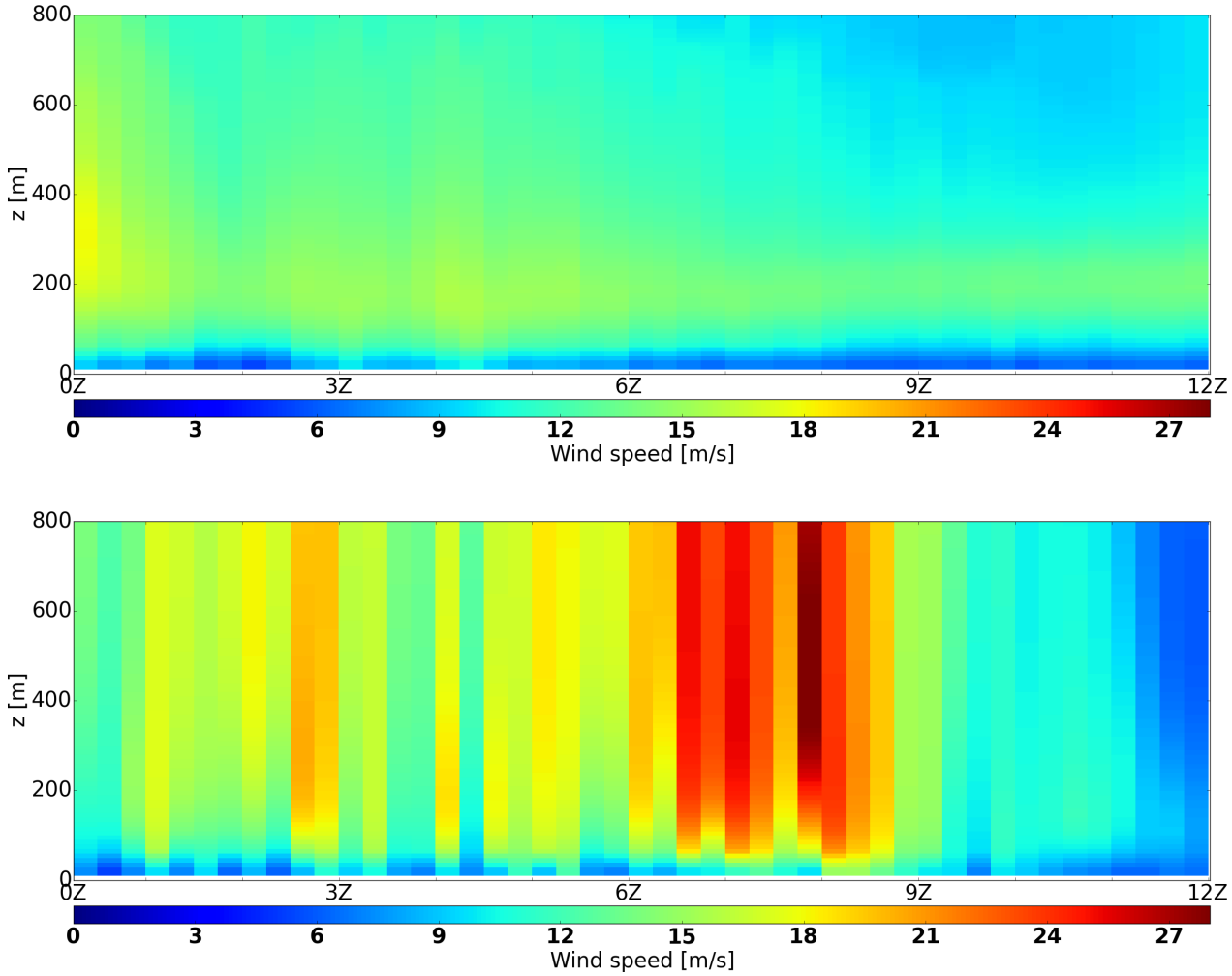

Figure 10. In the top panel, a 1-km horizontally spaced and 40-m vertically spaced grid was used to simulate the NLLJ. In the bottom panel, a 4-km horizontally spaced and 40-m vertically spaced grid was used.

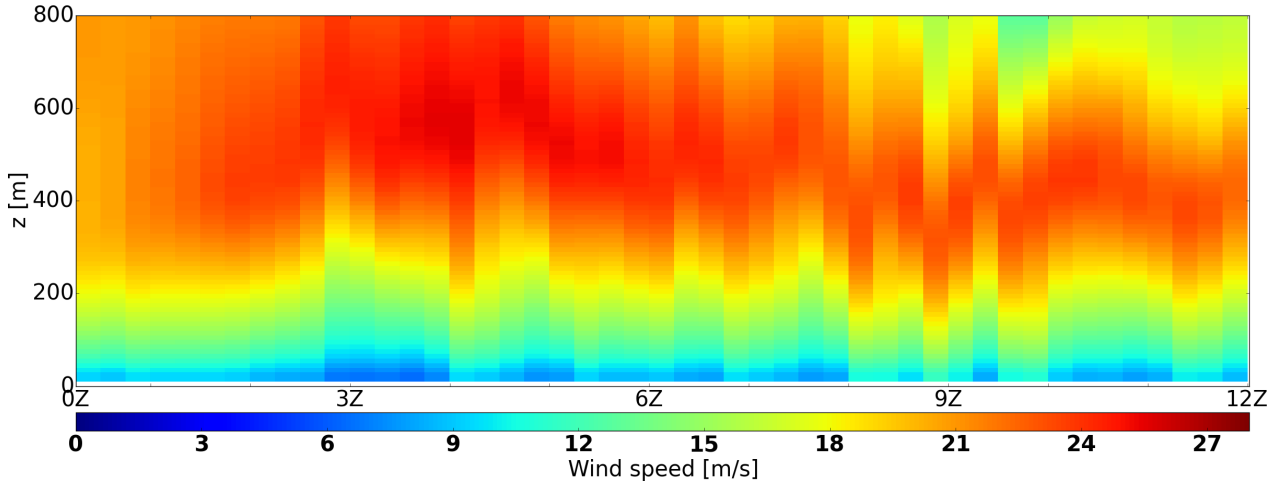

Figure 11. Wind field from WRF simulation on a 4-km horizontally spaced and 40-m vertically spaced grid using QNSE PBL parameterization.